Helicopter Performance Improvement with Variable Chord Morphing Rotors

Maryam Khoshlahjeh[+] Eui Sung Bae[†] Farhan Gandhi[‡]

Vertical Lift Research Center of Excellence (VLRCOE)
Department of Aerospace Engineering
The Pennsylvania State University
University Park, Pennsylvania, USA

Steven Webster[*]
AgustaWestland North America
Reston, Virginia 20190, USA

ABSTRACT

This study examines the effect of chord extention over a 20% spanwise section of the rotor blades of a utlity helicopter similar to the UH-60A Blackhawk. Chord extension is effectively realized by having a flat plate deploy through a slit in the trailing-edge between 63–83% span. For the helicopter simulation results in this paper, the Trailing-Edge Plate (TEP) is deployed 2 deg down relative to the airfoil chord line and results in a chord increase of 20% relative to the baseline airfoil chord. Since TEP extension changes the baseline SC-1094R8 airfoil profile, Navier-Stokes computational fluid dynamics is used to calculate the two-dimensional aerodynamic coefficients of the modified profile over a range of angles of attack and Mach number variations, and this is used in the helicopter performance simulations. The effect of TEP extension is examined, in particular, at moderate speed cruise condition (100 kts) and at high speed condition (140 kts), for variation in aircraft gorss weight and operating altitude. At both speeds, TEP extension allowed largest increases in aircrfat gross weight at high altitude (12,000 ft) – 2,200 lbs at 100 kts and 1,200 lbs at 140 kts. Alternatively, at the maximum gross weight of the baseline aircraft, TEP extension allowed power reductions of up to 15.3% at 100 kts, and in the range of 9.4% 12.7% at 140 kts. In stall dominated conditions (high gross weight, altitude and speed) where TEP extension is most effective, it singificantly reduces the blade section angles of attack on the retreating side, and although drag increases over spanwise regions where TEP is deployed, the overall reductions in drag due to change in rotor trim helps reduce power. While TEP extesnion leads to significant power reductions and gross wieght increases, increase in maximum speed is more modest (of the order of 10 kts at constant power, and approaching 20 kts albeit at much higher power requirement).

INTRODUCTION

One of the primary factors limiting the operating envelope of a rotorcraft is the onset of blade stall. Generally occurring at high speed on the retreating side of the rotor disk, or for high aircraft gross-weight and/or high altitude operation, stall leads to a loss in lift, sharp increase in drag and pitching moment, globally limits aircraft capability and induces high vibration and control loads. Alleviating stall is of much interest when operating close to the flight envelope boundaries, i.e., at high altitude, airspeed or high gross weight.

One approach to alleviating stall and expanding the helicopter's flight envelope is through the use of high-lift devices such as Gurney flaps or through the effective extension of blade chord. Such approaches, as well as the use of active trailing edge flaps and other devices have been previously examined in Refs. 1-6. Stall alleviation solutions focusing on the trailing-edge might be preferable to those that require leading-edge shape change (for e.g., leading-edge nose droop or leading-edge slats as examined in Ref. 5). This is because the aerodynamic pressures near the nose are much higher, requiring a stiffer structure and more actuation force, energy, and power to change shape.

Further, of the high-lift devices in the trailing-edge region, the Gurney flap has a high drag penalty (Refs. 1, 3). Consequently these would not be deployed on the advancing side of the rotor disk, which implies that high-frequency actuation (per rotor revolution) would be required. In Ref. 1 it was shown that statically extending the blade chord was effective in alleviating stall, reducing power requirement near the envelope boundaries, and/or expanding them. In fact, blade chord extension has several attractive features vis-à-vis the use Gurney flaps

[+]Graduate Research Assistant, mzk160@psu.edu
[†]Graduate Research Assistant, eub135@psu.edu
[‡] Professor, fgandhi@psu.edu
[*] VP, Research and Development, swebster@Awnainc.com

Proceedings of the 36th European Rotorcraft Forum, Paris, France, September 7-9, 2010.

as a high-lift device. For example, the drag penalty with chord extension would be lower than that associated with Gurney flap deployment. This allows chord extension to be implemented quasi-statically (changing from one flight condition to another, but not per rotor revolution). Further, actuation force requirements are fairly low (compared to trailing-edge flaps, for example, since overcoming aerodynamic hinge moments is not required).

Rotor blade chord extension can itself be realized in a number of different ways. One approach is to elastically deform the blade structure in the chordwise direction as examined in Ref. 6, and illustrated in Fig. 1. Alternatively, a thin splitting plate can be extended through a slit in the blade's trailing-edge over a certain spanwise section, as illustrated in Fig. 2. While the first approach would, in principle, lead to an aerodynamically cleaner profile, the energy requirement associated with elastically deforming the structure, as well as the requirement for flexible skins that can extend in-plane while carrying pressure out-of-plane, make this approach more challenging. The second alternative (using an extendable Trailing-Edge Plate, TEP) for helicopter applications was suggested in Ref. 1 by Leon et al., and appears to be a lower-risk technology. However, while Ref. 1 examined the performance benefits associated with blade chord extension, that study made the simplifying assumption that the aerodynamic lift and drag coefficients of the extended chord section were the same as those of the baseline airfoil. In effect, increment in lift (and drag) came about due to direct increase in chord area but change in airfoil profile was not accounted for.

The extension of the TEP through the slit, and the resulting change in airfoil profile would, in fact, be expected to change the sectional aerodynamic characteristics. In the current paper a Navier Stokes CFD solver is used to accurately calculate the aerodynamic coefficients of a rotor blade airfoil section with TEP extension. With these airfoil characteristics, the performance improvement and envelope expansion of a utility helicopter (similar to the UH-60A) is examined. Specifically, the benefits of using TEP extension over 20% blade span are evaluated at cruise and high-speed flight conditions, for variation in aircraft gross-weight and operating altitude, and appropriate conclusions are drawn.

ANALYSIS

In the present study, performance simulations are based on a utility helicopter with a 4-bladed articulated rotor similar to the UH-60A Blackhawk helicopter. The key properties of the baseline helicopter used are listed in Table 1. For the portions of the blade where there is no TEP, C81 tables (for the SC-1095 and SC-1094R8 airfoils) are used to obtain the sectional aerodynamic coefficients based on the local angle of attack and Mach number. The extendable TEP is situated between 63–83% spanwise location on each blade, and the baseline airfoil in this region is the SC-1094R8 airfoil. Aerodynamic coefficients are carefully evaluated using the 2D Navier-Stokes CFD code UM-TURNS (see Ref. 7) for the SC-1094R8 airfoil with TEP extensions of 10% and 20% of the baseline chord. However, studies showed that the benefits with 20% chord extension were always greater than those observed with 10% chord extension. Therefore, only 20% chord extension results are included in this paper. The TEP deployment angles considered relative to the airfoil chord line were 0 deg, 2 deg down and 4 deg down. Extending the TEP at 0 deg for the cambered SC-1094R8 airfoil, results in the effective reflexing of the airfoil along with a corresponding reduction in lift coefficient. Extending the TEP at 4 deg down, on the other hand, results in large nose-down pitching moments. TEP extension at 2 deg down, roughly parallel to the camber line, appeared to be the best compromise, whereby the lift coefficient did not decrease and the moment penalty was not as large. Although CFD simulations were carried out for all three deployment angles, the results in this paper are based only on a TEP deployment angle of 2 deg down relative to the airfoil chord line. CFD simulations for the baseline SC-1094R8 airfoil, as well as with TEP extensions were run over a range of airfoil angles of attack and Mach numbers that would be encountered over the flight envelope. The CFD computations were based on a 329x97 single block C-type grid, as shown in Fig. 3. The aerodynamic coefficients for the airfoil with TEP extension obtained as an output from the CFD simulations, C_l, C_d and C_m, are non-dimensionalized with respect to the extended chord. In the present study, a new set of aerodynamic coefficients, $\bar{C}_l$, $\bar{C}_d$ and $\bar{C}_m$, is obtained that is non-dimensionalized with respect to the *baseline chord length*, $\bar{c}$. These can be calculated as follows:

$$\bar{C}_l = (1 + \varepsilon/\bar{c})C_l$$

$$\bar{C}_d = (1 + \varepsilon/\bar{c})C_d \qquad (1)$$

$$\bar{C}_m = (1 + \varepsilon/\bar{c})^2 C_m$$

Where ε is the plate extension as a percentage of the baseline chord length, $\bar{c}$. Sample data for lift coefficient as a function of angle of attack at M=0.4 and M=0.7 are shown in Fig. 4, while corresponding drag polars are shown in Fig. 5. It is observed that while increasing $\bar{C}_{l-max}$, TEP extension does not result in a drag penalty at low $\bar{C}_l$ values – a major drawback observed with Gurney flaps (see Refs. 1, 3). For the blade sections with the extended trailing-edge plate, the sectional lift, L, drag, D, and moment, M, could then be calculated as follows:

$$L = \tfrac{1}{2}\rho V^2 \bar{c}\bar{C}_l$$

$$D = \tfrac{1}{2}\rho V^2 \bar{c}\bar{C}_d \qquad (2)$$

$$M = \tfrac{1}{2}\rho V^2 \bar{c}^2 \bar{C}_m$$

Alternatively, at any angle of attack and Mach number,

the *increments in aerodynamic coefficients ("deltas")* due to TEP extension could be extracted by subtracting the CFD calculated aerodynamic coefficients for the baseline SC-1094R8 airfoil (no TEP extension) from $\bar{C}_l$, $\bar{C}_d$ and $\bar{C}_m$ in Eq. 1. The sectional lift, drag, and moment can then be calculated by adding these extracted increments, $\Delta\bar{C}_l^{TEP}$, $\Delta\bar{C}_d^{TEP}$ and $\Delta\bar{C}_m^{TEP}$, to the experimentally obtained coefficients for the baseline SC-1094R8 airfoil from C81 tables. Thus,

$$L = \tfrac{1}{2}\rho V^2 \bar{c}(C_{l-base}^{C81} + \Delta\bar{C}_l^{TEP})$$

$$D = \tfrac{1}{2}\rho V^2 \bar{c}(C_{d-base}^{C81} + \Delta\bar{C}_d^{TEP}) \qquad (3)$$

$$M = \tfrac{1}{2}\rho V^2 \bar{c}^2(C_{m-base}^{C81} + \Delta\bar{C}_m^{TEP})$$

Such an approach of adding "increments" for high-lift devices or active sections to the baseline coefficients from C81 tables is commonly followed in rotorcraft research (see for example, Refs. 2, 3, 5, 8 and 9), and is adopted in the present study as well. Non-dimensionalizing the aerodynamic coefficients with respect to the baseline chord (as shown in Eq. 1) allows convenient implementation of this approach. Further, it also facilitates easy comparison of the aerodynamic coefficients with TEP extension to those obtained with trailing-edge flap deflection, Gurney flap deployment, etc. (which do not involve any change in airfoil chord).

The aerodynamic model also includes a lifting line vortex wake model with prescribed geometry (Ref. 10). The wake-induced velocity at the aerodynamic integration points along the blade span are calculated by using the Biot-Savart law, accounting for the contribution of each vortical element. As the TEP is extended, the lift increases locally. This causes the strength of the bound vorticity, as well as the trailed vorticity at the edges of that TEP to change which, in turn, changes the inflow distribution. Accounting for the change in vortex strength and inflow due to TEP extension allows for a more accurate calculation of the induced power as well as profile power. Since the current study focuses on moderate speed cruise and high speed flight conditions, but not low speed flight, the self-induced distortions in wake geometry prominent at low speeds are less important and a prescribed wake is considered sufficient.

The blades are modeled as undergoing rigid flap rotations about the offset flapping hinge but lag and torsion deformation is neglected in the analysis. This model was first developed and validated for use in Ref. 11, and has also been used in Refs. 1, 2, 3, 8, 9, and 12. With a good aerodynamic model it is quite appropriate for trim and power predictions. The baseline power predictions (without TEP), versus airspeed, compared well with CAMRAD-II predictions as well as flight test data of a UH-60A helicopter (see Ref. 11). Further, such a rigid blade analysis can be a good choice in parametric design studies requiring a large number of simulations. Since the study does not focus on loads and vibrations, modeling elastic deformations of the blades would not be considered critical. However, the extension of the TEP does increases nose-down pitching moments (Fig. 6), and thus torsional flexibility in the blades (and the lack thereof in the analysis used in this study) could have an effect on the results. To assess the implication of this simplifying assumption, the model was also set up in RCAS (Ref. 13) with the blades undergoing (a) rigid flapping only, and (b) rigid flapping along with elastic twist. For both, options (a) and (b), required power versus airspeed was calculated without TEP extension as well as with 20% TEP extension. Figure 7 shows that at moderate gross weight (18,300 lbs) and low altitude operations, the rigid blade approximation is quite appropriate. Further, TEP extension in this nonstall dominated condition actually increases power requirement slightly due to the profile power drag of the extended TEP. Figure 7 also shows that at higher gross weight and altitude the blade sections are closer to stall, pitching moments are larger, and torsional flexibility has an important effect. With no TEP extension, the torsionally compliant model has lower power requirement than the torsionally rigid model since the nose-down twist reduces the angles of attack in the outboard sections. More interesting and relevant, though, is the question of how power reductions due to TEP extension compare when using the two models. The results indicate that the power reductions with the torsionally elastic model are slightly smaller than those predicted with the torsionally rigid model. With that consideration, the results presented in this paper should regarded as the upper limits on benefits that TEP extension would offer.

The UH-60A helicopter model is propulsively trimmed at the different conditions examined in this paper, both with and without TEP extension, to assess the benefits that TEP extension offers. In particular, the paper focuses on two flight speeds (100 kts cruise flight, and 140 kts high speed flight), altitude variation from sea level up to 12,000 ft, and gross weight variation from 16,000 lbs up to 28,000 lbs.

RESULTS

Figure 8 shows rotor power versus gross weight at 100 kts cruise condition. Results are shown for several different altitudes. At sea level, there is no advantage to using chord extension. As altitude increases the helicopter would operate at increasing rotor collective pitch and be more susceptible to stall. This limits the maximum gross weight of the helicopter at high altitude. Given the available power, the use of chord extension can significantly increase the high lift capability at high altitude. For example, at 12,000 ft altitude, the maximum gross weight of the baseline helicopter is around 20,500 lbs. The helicopter is unable to generate enough thrust to allow a higher gross weight. In contrast, with chord extension, the maximum gross weight now increases to 22,700 lbs, a 2,200 lb increase in payload capability over the baseline. The corresponding required power at 12,000

ft is 2081 HP. An engine rated at 3,000 HP at sea level, just about provides this required power at 12,000 ft. At 8,000 ft altitude, the maximum gross weight of the baseline helicopter is around 24,000 lbs. The helicopter is unable to generate enough thrust to allow a higher gross weight. With chord extension, the maximum gross weight now increases to 25,000 lbs, giving a smaller 1,000 lb increase in payload capability at this lower altitude. The corresponding required power at 8,000 ft is 2,127 HP. For an engine rated at 3,000 HP at sea level, the available power at 8,000 ft is 2,360 HP which is greater than that required for the configuration with trailing edge extension. From the figure, as the maximum gross weight (or payload capability) for high altitude operation decreases, chord extension technology is seen to be most effective. At 4,000 ft, large reduction in power requirement is observed at high gross weight. Although the baseline aircraft can generate sufficient lift, it operates close to stall at very high gross weights. The use of chord extension in such cases reduces the angles of attack, alleviates stall and thereby reduces rotor drag and power requirement. For example, at 4,000 ft, 28,000 lbs gross weight, the power requirement for the baseline aircraft is 2,767 HP. Using chord extension reduces power requirement to 2,343 HP, a 15.3% reduction over the baseline.

Figure 9 shows rotor power versus gross weight at 140 kts, high speed condition. As in Fig. 8, results are shown for several different altitudes. Unlike the 100 kts case, increase in maximum gross weight is realized at all altitudes, although the effect increases with increasing altitude. The actual increases in gross-weight capability are smaller than those observed in cruise. For example, at 12,000 ft altitude, the maximum gross weight of the baseline helicopter is around 18,800 lbs. The helicopter is unable to generate enough thrust to allow a higher gross weight. In contrast, with chord extension, the maximum gross weight now increases to 20,000 lbs, assuming available power – a 1,200 lb increase in payload capability over the baseline (compared to a 2,200 lb increase at 100 kts). The corresponding required power at 12,000 ft is 2527 HP. For an engine rated at 3,000 HP at sea level, the available power at 12,000 ft would be only be 2080 HP. At this available power the increase in gross-weight over the baseline would be a more modest 500 lbs. On the other hand with an engine rated at 4,000 HP at sea level, the available power at 12,000 ft would be 2,772 HP, which is larger than that required and TEP extension could realize the 1,200 lbs gross weight increase. At 8,000 ft altitude, the maximum gross weight of the baseline helicopter is around 22,000 lbs. With chord extension, the maximum gross weight now increases to 23,000 lbs, albeit at a significantly higher power requirement. If the available power constraints are considered (even assuming an engine rated at 4,000 HP at sea level), the increase in maximum gross weight is only around 700 lbs. On the other hand, at 22,000 lb gross weight, use of TEP extension results in a 370 HP or 12.7% reduction in power requirement over the baseline power requirement of 2,906 HP (see points marked A and B on Fig. 9). At 4,000 ft altitude and maximum gross weight of 24,500 lbs for the baseline aircraft, using chord extension results in a 10.9% reduction in power requirement (from 3,111 HP to 2,772 HP). Finally at sea level and a maximum gross weight of 27,500 lbs for the baseline aircraft, using chord extension results in a 9.4% reduction in power requirement (from 3,586 HP to 3,250 HP).

Next, the mechanism of power reduction is examined in greater detail. At 140 kts airspeed, 8,000 ft altitude, consider points A and B marked on Fig. 9. Both correspond to a gross-weight of 22,000 lbs and the TEP extension was previously reported to result in a 12.7% power reduction. Figure 10 shows the difference in lift between the baseline and the extended chord configuration. As can be expected, there is an augmentation in the lift over the annulus from 63% to 83% of the blade radius, due to TEP extension. Since the aircraft is trimmed to the same thrust as the baseline, the additional lift associated with TEP extension is accompanied by a drop in collective from 12.54 deg for the baseline aircraft to 11.2 deg for the configuration with TEP extension. The angles of attack for the two configurations are presented in Figs. 11a and 11b. The baseline configuration in Fig. 11a is in deep stall on the retreating side of the disk. Figure 11b shows how the lower collective on the configuration with TEP extension reduces the angles of attack on the retreating side. As a result of the reduced angles, the sectional drag is reduced over most of the rotor disk. Only where TEP extension is present is a slight increase in profile drag observed. The drag difference between the baseline and the configuration with TEP extesnion is presented in Fig. 12. The large reduction in drag in the region of the blade tips, especially on the retreating side and at the rear of the disk, is particularly effective in reducing main rotor torque and power.

Figure 13 shows the rotor power versus airspeed for an aircraft gross weight of 24,000 lbs, at 8,000 ft altitude. The maximum speed for the baseline aircraft is observed to be 110 kts. With TEP extension, the maximum speed can increase to 128 kts, albeit at a higher power requirement. At increasing speeds, larger reductions in power are available with TEP extension, vis-à-vis the baseline aircraft. At the maximum speed of the baseline aircraft, TEP extension results in a power reduction of 12% (from 2,355 HP for the baseline to 2,068 HP for the configuration with TEP extension). As regards the increase in maximum speed, the 18 kt increase cited above can only be realized with the engine rated at 4,000 HP at sea level. With an engine rated at 3,000 HP at sea level, the maximum available power at 8,000 ft would only be 2,360 HP, and the corresponding increase in maximum speed with chord extension is 10 kts over the baseline.

It should be noted that the benefits observed in this

section are dependent on the spanwise location of the extendable TEP. In the present study, the maximum outboard location was set at 83% since the airfoil changed from the SC-1094R8 to the SC-1095 beyond this location, and CFD-based two-dimensional airfoil coefficients with TEP extension were only obtained for the SC-1094R8 airfoil. In Ref. 1, however, a more outboard location was seen to yield larger benefits compared to those reported in the current study.

CONCLUSIONS

This study examines the effect of chord extention over a 20% spanwise section of the rotor blades of a utlity helicopter similar to the UH-60A Blackhawk. Chord extension is effectively realized by having a flat plate deploy through a slit in the trailing-edge between 63–83% span. For the helicopter simulation results in this paper, the Trailing-Edge Plate (TEP) is deployed 2 deg down relative to the airfoil chord line and results in a chord increase of 20% relative to the baseline airfoil chord. Since TEP extension changes the baseline SC-1094R8 airfoil profile, Navier-Stokes computational fluid dynamics is used to calculate the two-dimensional aerodynamic coefficients of the modified profile over a range of angles of attack and Mach number variations, and this is used in the helicopter performance simulations. The effect of TEP extension is examined, in particular, at moderate speed cruise condition (100 kts) and at high speed condition (140 kts), for variation in aircraft gorss weight and operating altitude. The conclusions that were drawn from the present study are summarized below.

At moderate cruise speed (100 kts), there is not much benefit to deploying the TEP (effectively extending chord) at sea level. At higher altitudes however, the maximum gross weight of the aircraft can increase with TEP extension, with an increase of up to 2,200 lbs observed at 12,000 ft altitude. At 4,000 ft altitude, at a gross-weight correponding to the maximum for the baseline aircraft, TEP extension resulted in a power reduction of 15.3%.

In high speed cruise (140 kts), the increases in gross-weight capability are somewhat smaller than those observed in cruise. For example, the largerst increase in aircraft gross-weight at high altitude (12,000 ft) is 1,200 lbs, vis-a-vis the baseline aircraft. At sea level, 4,000 ft and 8,000 ft altitude, at gross-weights correponding to the maximum for the baseline aircraft, TEP extension resulted in power reductions ranging from 9.4% to 12.7%.

Examining the blade sectional angles of attack around the rotor disk in stall dominated conditions (high gross weight, altitude and speed) revealed that the angles of attack on the retreating side decreased significantly with TEP extension, with the rotor collective pitch correspondingly reducing from 12.54 deg to 11.2 deg. Blade section drag is seen to increase in the region where TEP is deployed (due to increase in profile drag), but large reductions in drag at the blade tip, especially on the retreating side and the rear of the disk result in overall power reductions.

At high altitude and gross weight, increase in maximum speed with TEP extension is modest (of the order of 10 kts at constant power, and approaching 20 kts albeit at much higher power requirement). On the other hand, at the maximum operating speed of the baseline aircraft, power reduction of the order of 12% is observed.

REFERENCES

[1] Leon, O., Hayden, E., and Gandhi, F., "Rotorcraft Operating Envelope Expansion Using Extendable Chord Sections," *Proceedings of the 65th Annual AHS International Forum and Technology Display*, Grapevine, Texas, May 27-29, 2009.

[2] Bae, E.-S., Gandhi, F., Maughmer, M., "Optimally Scheduled Deployment of Gurney Flaps for Rotorcraft Power Reduction," Proceedings of the 65th Annual Forum of the American Helicopter Society, Grapevine, Texas, May 27-29, 2009.

[3] Bae, E.-S., and Gandhi, F., "Optimally Actuated Spanwise-Segmented Aerodynamic Effectors for Rotorcraft Power Reduction," *Proceedings of the 66th Annual Forum of the American Helicopter Society*, Phoenix, Arizona, May 11-13, 2010.

[4] Maughmer, M., Lesieutre, G., and Kinzel, M., "Miniature Trailing-Edge Effectors for Rotorcraft Performance Enhancement," AHS 61st Annual Forum, Grapevine, TX, June 2005.

[5] Yeo. H., "Assessment of Active Controls for Rotor Performance Enhancement," Journal of the American Helicopter Society, Vol. 53, (2), April 2008, pp. 152-163.

[6] Barbarino, S., Gandhi, F., and Webster, S., "Design of Extendable Chord Sections for Morphing Helicopter Rotor Blades," *Proceedings of the ASME 2010 Conference on Smart Materials, Adaptive Structures and Intelligent Systems, SMASIS2010*, Philadelphia, Pennsylvania, Sept. 28 – Oct. 1, 2010, SMASIS2010-3668

[7] Jose, A.I., Sitarman, J., and Baeder, J.D., "An Investigation into the Aerodynamics of Trailing Edge Flap and Flap-Tab Airfoils Using CFD and Analytical Methods," *63rd Forums of the American Helicopter Society International*, Virginia Beach, VA, May 1-3, 2007.

[8] Leon, O., Gandhi, F., " Rotor Power Reduction using Multiple Spanwise-Segmented, Optimally-Actuated Trailing-Edge Flaps," ERF 35th Annual Forum, Hamburg, Germany. September 22-25, 2009.

[9] Duling, C., Gandhi, F., and Straub, F., "On Power and Actuation Requirements in Swashplateless Primary Control using Trailing-Edge Flaps,"

Proceedings of the 66th Annual Forum of the American Helicopter Society, Phoenix, Arizona, May 11-13, 2010.

[10] Leon, O., "Reducing Helicopter Main Rotor Power Requirements using Multiple Trailing Edge Flaps and Extendable Chord Sections," Master's Thesis, The Pennsylvania State University, University Park, 2009.

[11] Bluman, J., Gandhi, F., "Reducing Trailing Edge Flap Deflection Requirements in Swashplateless Primary Control with a Moveable Horizontal Tail," Proceedings of the 65th Annual Forum of the American Helicopter Society, Grapevine, Texas, May 27-29, 2009.

[12] Steiner, J., Gandhi, F., Yoshizaki, Y., "An Investigation of Variable Rotor RPM on Performance and Trim," Proceedings of the 64th Annual Forum of the American Helicopter Society, Montreal, Canada, April 29 – May 1, 2008.

[13] Saberi, H., Khoshlahjeh, M., Ormiston, R. and Rutkowski, M. "Overview of RCAS and Application to Advanced Rotorcraft Problems," Proceedings of the American Helicopter Society 4th Decennial Specialists' Conference on Aeromechanics, San Francisco, California, January 21-23, 2004.

Table 1. Key UH-60A Helicopter Properties.

Parameter	Symbol	Value
Rotor Radius	R	26.83 ft
Angular Velocity	Ω	27 rd/s
Blade Root Cutout	R_{co}	3.83 ft
Blade Chord*	c	1.73 ft
Blade Twist*	θ_{tw}	-16°
Blade Solidity	σ	.0822
Flapping moment of inertia	I_β	1618 slug.ft^2
Rotor Blade Airfoil*		SC-1095 SC-1094R8
Shaft Forward Tilt	α_{Sx}	3°
Tail Rotor Cant Angle	φ_{TR}	20°
Longitudinal CG Offset+	x_{cg}	1.525 ft
Lateral CG Offset+	y_{cg}	0 ft
Vertical CG Offset+	z_{cg}	-5.825 ft
Lon. Stabilator offset+	x_{ht}	29.925 ft
Lat. Stabilator offset+	y_{ht}	0 ft
Vert. Stabilator offset+	z_{ht}	-5.915 ft
Lon. Tail Rotor offset+	x_{tr}	32.565 ft
Lat. Tail Rotor offset+	y_{tr}	0 ft
Vert. Tail Rotor offset+	z_{tr}	0.805 ft

* Varies span-wise + Distance wrt the hub

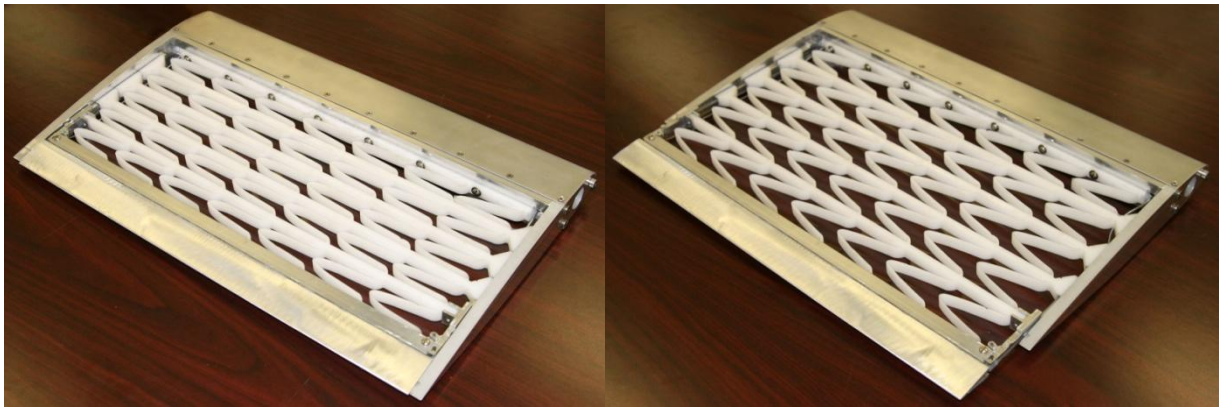

Figure 1: Chord extension through elastic deformation of structure (from Ref. 6) in contracted (left), and extended (right) configurations (without skin)

Figure 2: Chord increase through the use of extendable Trailing-Edge Plate (TEP) shown in retracted (above), and extended (below) configurations (top skin removed in figure)

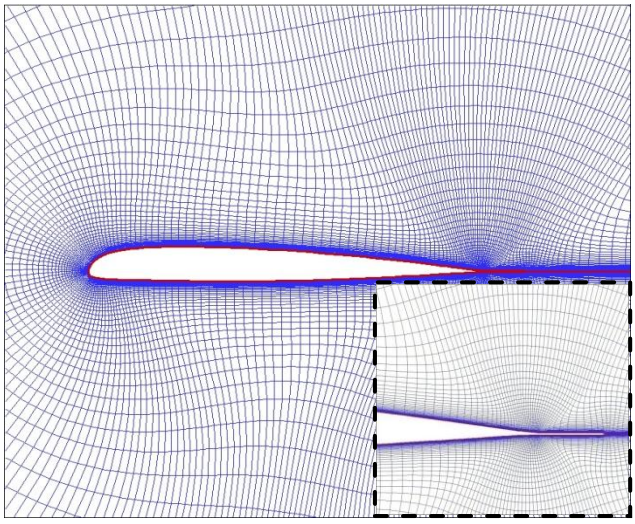

Figure 3: CFD single block C type grid for SC1094R8 airfoil with extended Trailing-Edge Plate

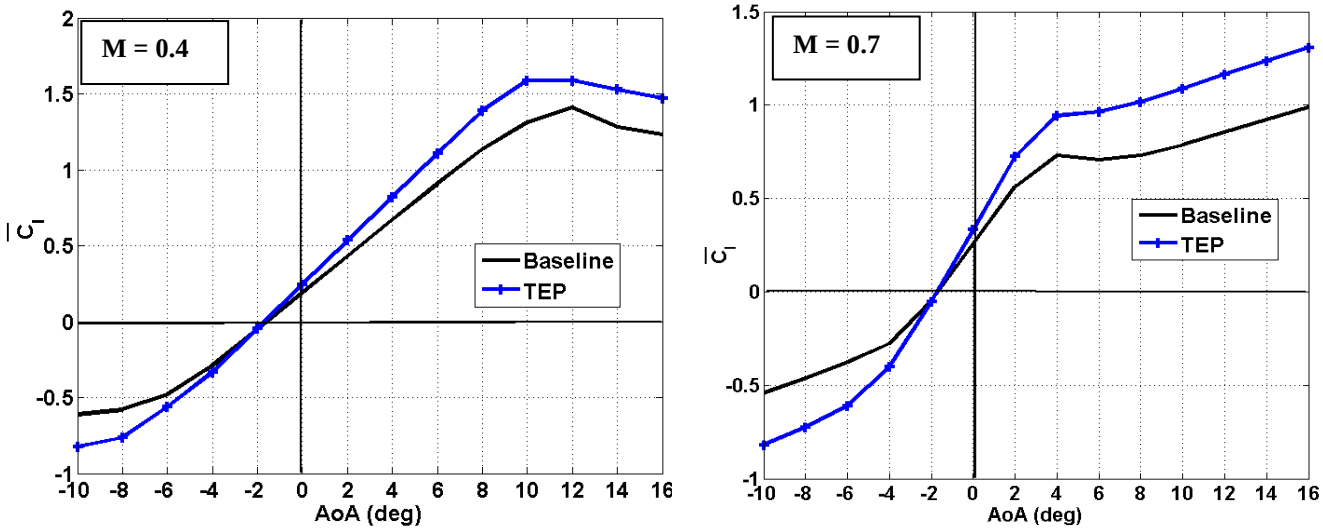

Figure 4: Lift coefficient comparison for baseline SC1094R8 and airfoil with TEP at Mach No. = 0.4 (left), and Mach No. = 0.7 (right)

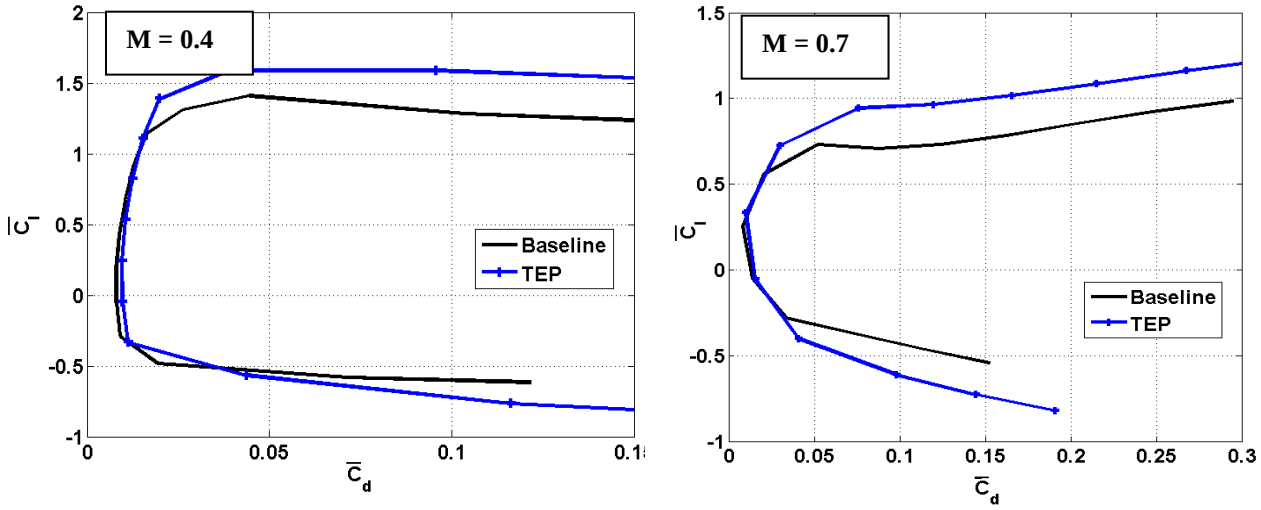

Figure 5: Drag polar comparison for baseline SC1094R8 airfoil and airfoil with TEP, (a) at Mach No. = 0.4 (left), and Mach No. = 0.7 (right)

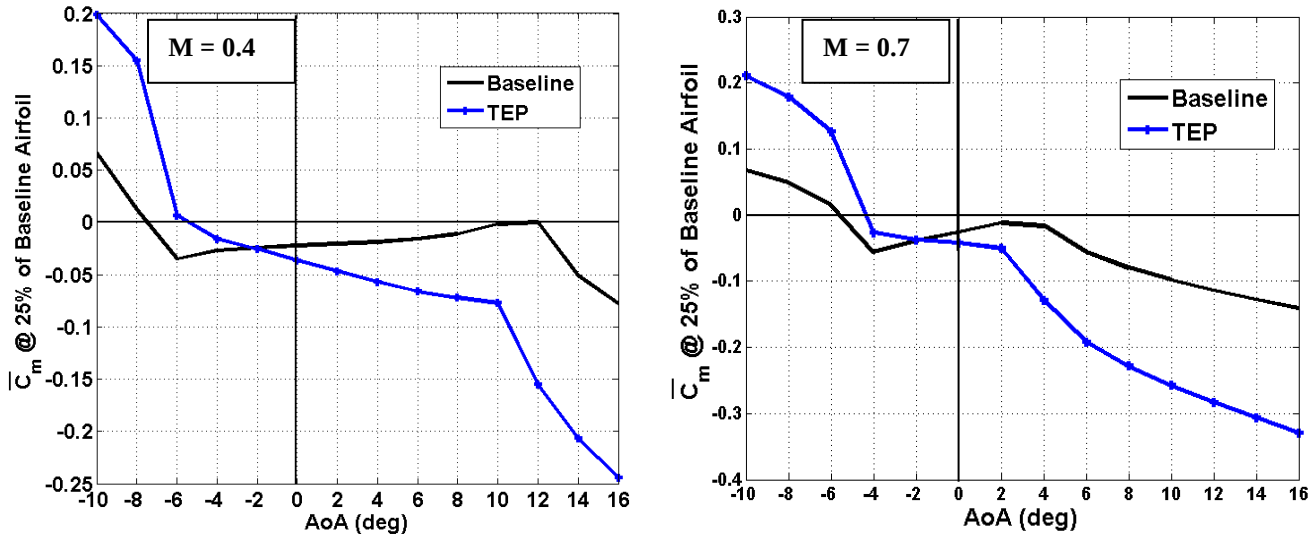

Figure 6: Moment coefficient comparison for baseline SC1094R8 airfoil and airfoil with TEP at Mach No. = 0.4 (left), and Mach No. = 0.7 (right)

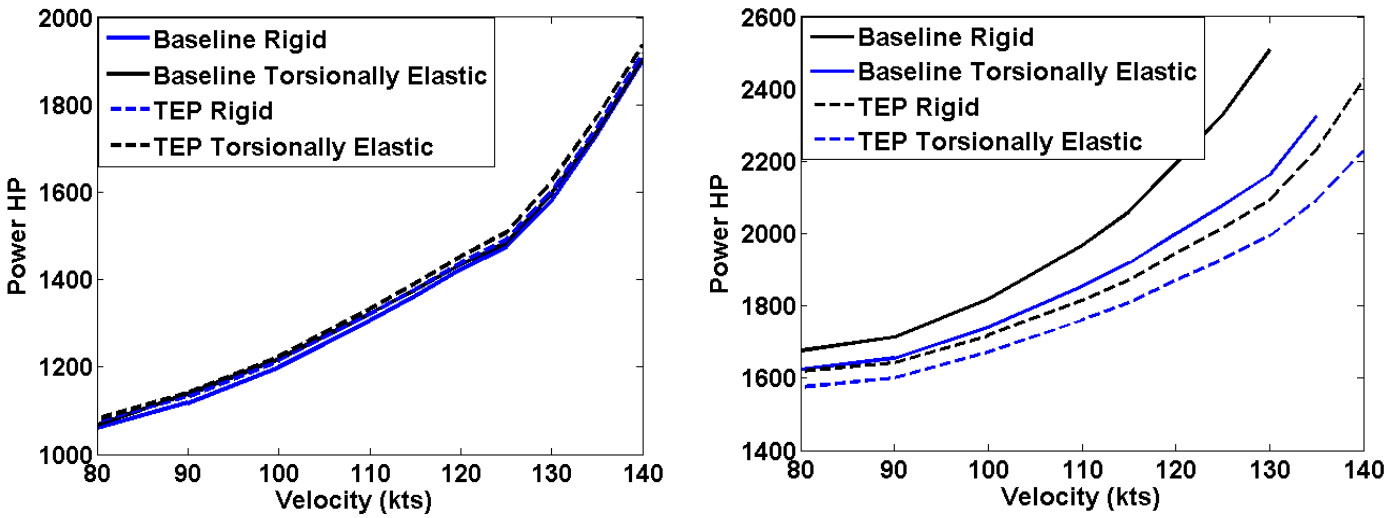

Figure 7: Power predictions using rigid blade and torsionally elastic blade models at sea level, 18300 lbs gross weight (left), and 4,000 ft, 24000 lbs gross weight (right)

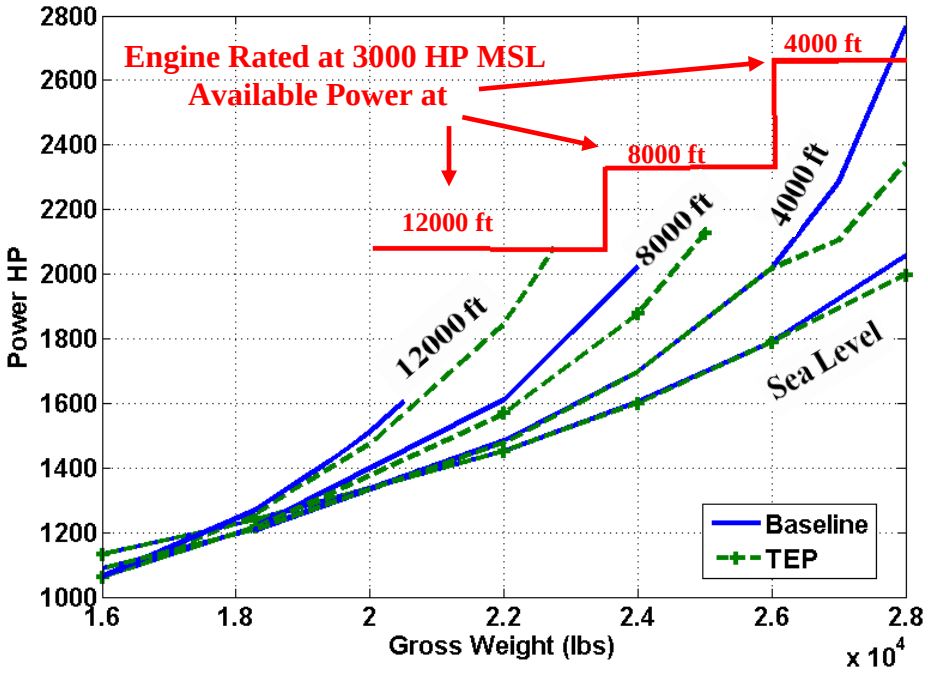

Figure 8: Power requirement versus gross weight at 100 kts, results for baseline as well as configuration with TEP extension, at different altitudes

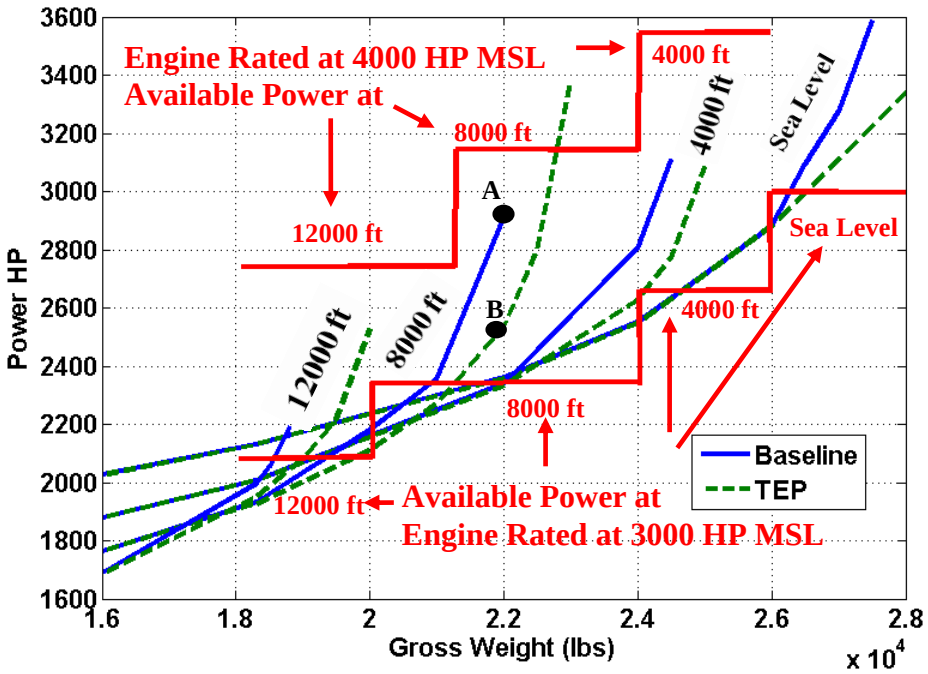

Figure 9: Power requirement versus gross weight at 140 kts, results for baseline as well as configuration with TEP extension, at different altitudes

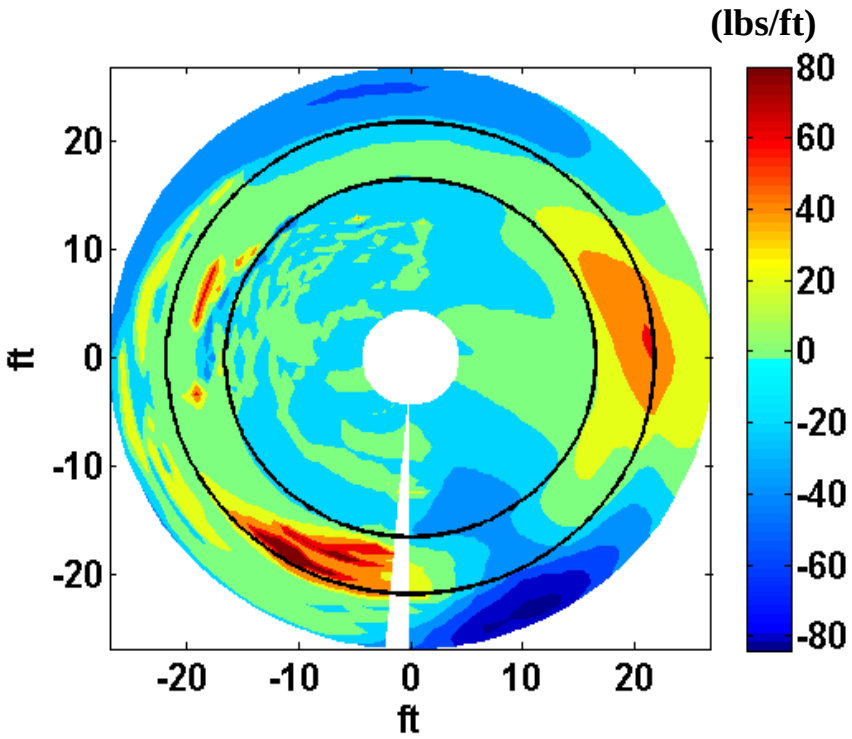

Figure 10: Lift difference (lbs/ft) between configuration with TEP and baseline configuration at 8,000 ft altitude and 22,000 lbs gross weight, 140 knots

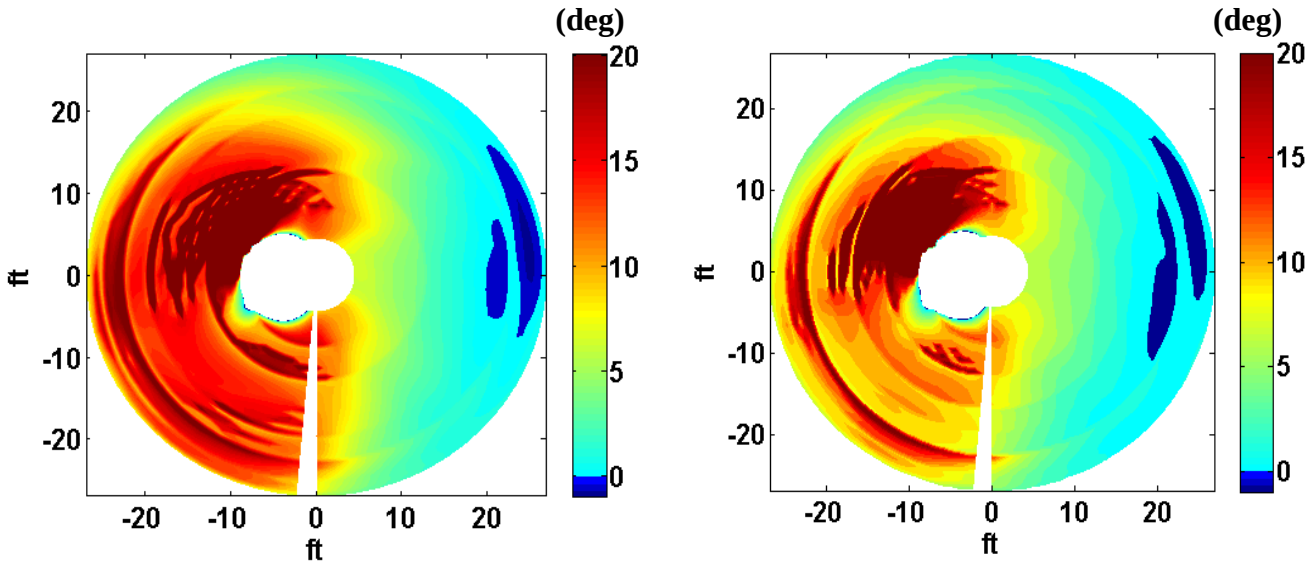

Figure 11: Angle of attack (deg) for baseline (left) and configuration with TEP (right) at 8,000 ft altitude, 22,000 lbs gross weight, 140 knots

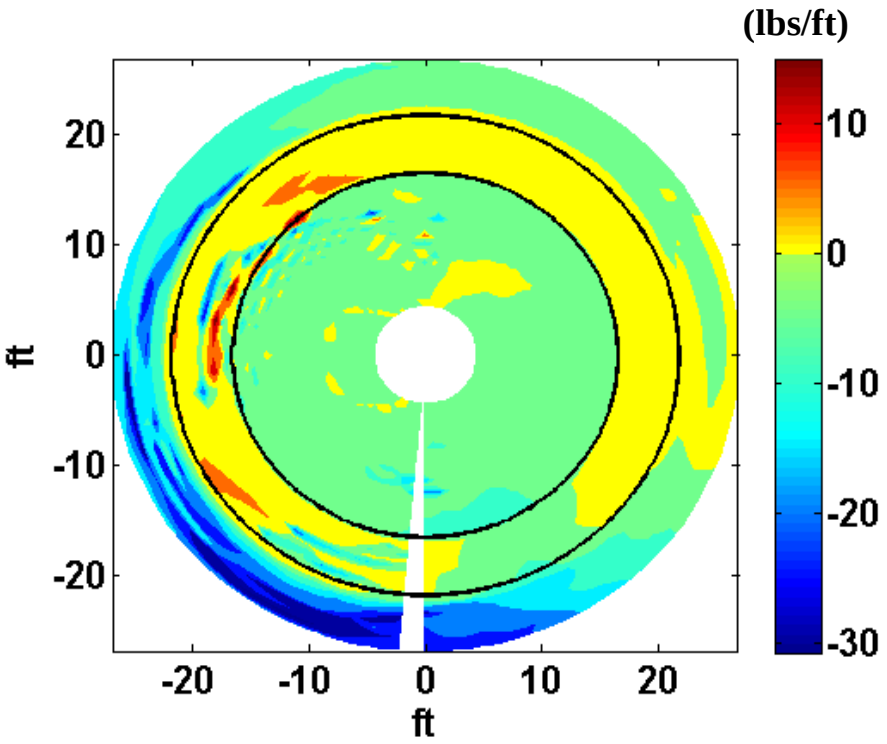

Figure 12: Drag difference (lbs/ft) between configuration with TEP and baseline configuration at 8,000 ft altitude and 22,000 lbs gross weight, 140 knots

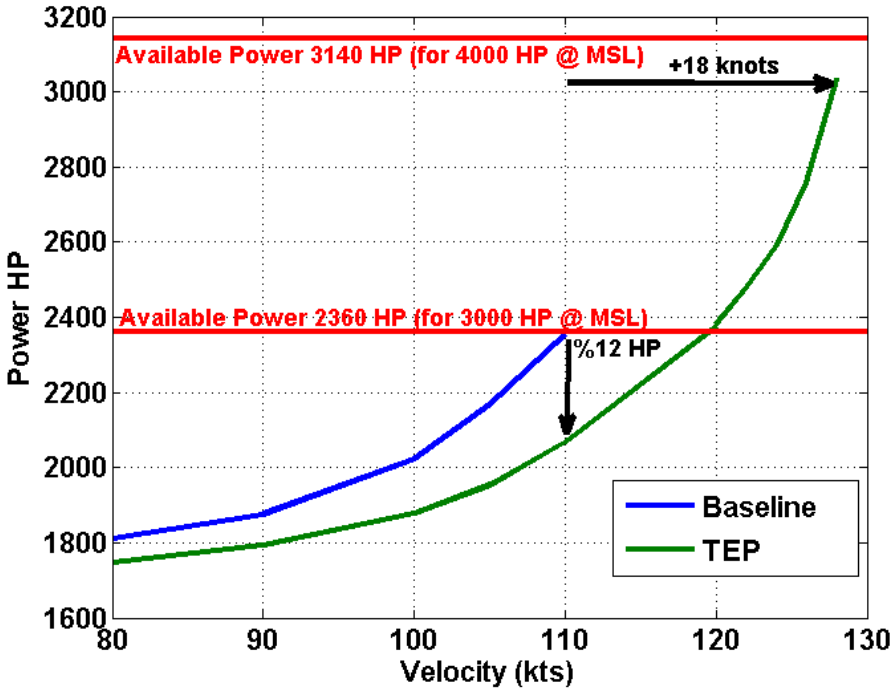

Figure 13: Power versus airspeed for baseline as well as configuration with TEP at 8,000 ft altitude, 24,000 lbs gross weight